Supramolecular Chemistry
Publication details, including instructions for authors and subscription information:
http://www.informaworld.com/smpp/title~content=t713649759

Pyrene bichromophores composed of polyaminopolycarboxylate interlink: pH response of excimer emission

Lorena Machi[a]; Iliana C. Muñoz[a]; Refugio Pérez-González[a]; Mario Sánchez[b]; Motomichi Inoue[a]
[a] Departamento de Investigación en Polímeros y Materiales, Universidad de Sonora, Hermosillo, Sonora México [b] Centro de Investigación en Materiales Avanzados, Apodaca, Nuevo León México

To cite this Article Machi, Lorena , Muñoz, Iliana C. , Pérez-González, Refugio , Sánchez, Mario and Inoue, Motomichi(2009) 'Pyrene bichromophores composed of polyaminopolycarboxylate interlink: pH response of excimer emission', Supramolecular Chemistry, 21: 8, 665 — 673
To link to this Article: DOI: 10.1080/10610270802709360
URL: http://dx.doi.org/10.1080/10610270802709360

Supramolecular Chemistry
Vol. 21, No. 8, December 2009, 665–673

Taylor & Francis
Taylor & Francis Group

Pyrene bichromophores composed of polyaminopolycarboxylate interlink: pH response of excimer emission

Lorena Machi[a]*, Iliana C. Muñoz[a], Refugio Pérez-González[a], Mario Sánchez[b] and Motomichi Inoue[a]

[a]*Departamento de Investigación en Polímeros y Materiales, Universidad de Sonora, Hermosillo, Sonora México;* [b]*Centro de Investigación en Materiales Avanzados, Apodaca, Nuevo León México*

(*Received 10 August 2008; final version received 15 October 2008*)

Fluorescent response to pH has been studied on water-soluble pyrene-based bichromophores, (edtapy)H_2 and (dtpapy)H_3, in which two pyrenyl groups are linked by an ethylenediaminetetraacetate (EDTA) and a diethylenetriaminepentaacetate (DTPA) unit, respectively, through amide linkages. The excimer emission of the EDTA derivative is strengthened sharply with increasing pH at two steps; the first step is associated with the dissociation of acidic hydrogen from amino nitrogen in partially protonated species (edtapy)H^- and the second step is attributable to the amide group. The excitation spectra have evidenced the formation of a static excimer in the ground state of completely deprotonated species (edtapy)$^{2-}$. The close contact between pyrenyl groups in (edtapy)$^{2-}$ has been confirmed by density functional theory, which has also shown that the close contact is broken when amino nitrogen is protonated. The DTPA derivative exhibits a strong excimer emission, which shows an intensity–pH profile of an 'off–on–off–on' type. This rare pH response is ascribable to multiple protonation sites in the DTPA chain, as confirmed by ^{1}H NMR. The novel pH-sensing capabilities in specific pH regions are due to the combination of the fluorescent group with the polyaminopolycarboxylate chains whose conformations are reversibly altered by protonation–deprotonation processes.

Keywords: bichromophores; DTPA; EDTA; fluorescence; pH sensors; pyrene derivatives

Introduction

Molecular sensors (or chemosensors) are composed of an ionophore (as a cation-binding site) and a fluorophore (as a signalling subunit), and can readily reach a very low detection limit by means of fluorimetric techniques (*1–3*). When such a fluoroionophore contains two identical fluorophores whose mutual distance can be altered upon complexation with a cation, excimer formation may be either facilitated or hindered so that the recognition towards the cation can be monitored by excimer emission. Its sensitivity to an environmental change is higher than that of the corresponding monomeric chromophore. Another advantage of bichromophores is that a ratiometric method based on the excimer-to-monomer intensity ratio permits self-calibration in practical applications. Examples of bichromophoric metal sensors have been reported for linear polyamines and polyethers bearing naphthalene, anthracene or pyrene fragments as chromophores at the chain ends (*4–14*). Especially, pyrene provides excellent luminescent chemosensors based on excimer emission because of its features such as a high quantum yield of fluorescence emission, a long lifetime of the excited state and an efficient excimer formation in comparison with other polyaromatic chromophores (*9–11*). As sensors useful in aqueous systems, however, pyrene derivatives normally have too low a water solubility because of the high hydrophobicity of pyrene. Only a few bis(pyrenyl)-polyamine bichromophores have been reported to be water soluble (*15*, *16*). Among them, the diethylenetriamine derivative alone exhibits a well-defined excimer emission. Its intensity is very low at pH in acidic region and is greatly enhanced with the increase in pH; this pH response represents an 'off–on' intensity profile against the pH window. Addition of acetonitrile into the aqueous solution of the bichromophore at increasing concentrations (0–50%) enhances the intensity, and its pH dependence exhibits 'off–on–off' and 'off–on–off–on' profiles (*16*). Such a novel fluorescence intensity profile against pH window attracts particular attention in connection with the highly demanded pH sensors capable of detecting even a small pH change in a specific region. A critical factor for molecular design of pH-sensing bichromophores is the selection of the interlinking chains that involve appropriate electron-donor sites and have a suitable length. Another obvious factor is that hydrophobic derivatives should be made soluble in water by introducing hydrophilic groups into interlinking chains. These requirements are expected to be satisfied by ethylenediaminetetraacetate (EDTA), which is a typical polyaminopolycarboxylate, as reported for

*Corresponding author. Email: lmachi@polimeros.uson.mx

ISSN 1061-0278 print/ISSN 1029-0478 online

DOI: 10.1080/10610270802709360
http://www.informaworld.com

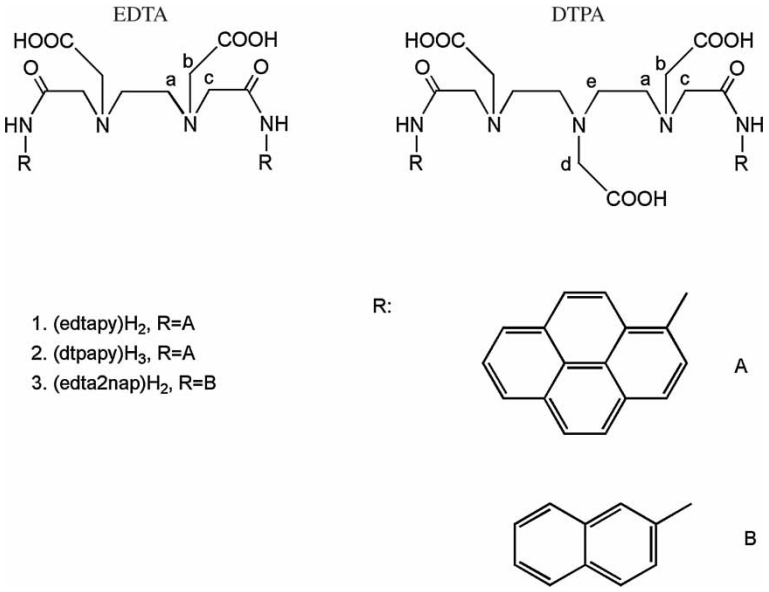

Scheme 1. Bichromophores composed of EDTA or DTPA interlink.

naphthalene-based bichromophores (*17*, *18*); the conformation of the polyamino chain may be changed with pH, and the anionic carboxylate arms may endow a pyrene derivative with water solubility (*19*, *20*). These characteristics will be more pronounced in diethylenetriaminepentaacetate (DTPA), which bears a larger number of amino and carboxyl groups. In this work, therefore, we have employed EDTA and DTPA as an interlinking chain to design pyrene-based bichromophores **1** and **2** in Scheme 1, abbreviated as (edtapy)H_2 and (dtpapy)H_3, respectively, with acidic hydrogen. These bichromophores exhibit an intense excimer emission, which sensitively responds to pH with a rare intensity–pH profile. The novel pH response has been consistently interpreted by excitation spectra, ^{1}H NMR and density functional theory (DFT) calculations.

Results and discussion

Luminescence of (edtapy)H_2

A reaction between EDTA dianhydride and 1-aminopyrene gave a 1:2 addition product (edtapy)H_2 (**1** in Scheme 1). The resulting bichromophore was soluble enough in water for luminescence experiments over the entire pH range studied, although the water solubility ($< 0.1\,\mathrm{mmol\,kg^{-1}}$) was too low for the ^{1}H NMR measurements even in the pH range where anionic species $(\mathrm{edtapy})^{2-}$ is present with complete deprotonation.

Figure 1 shows the emission spectra at different pH values. Basic solutions exhibited an intense structureless band at 480 nm and weak bands with vibronically structured features between 370 and 420 nm. The former emission is assignable to pyrene excimer, while the latter to monomeric (or isolated) pyrene (*11*, *15*, *16*, *21*). As pH was lowered, the intensity of the excimer band was rapidly reduced to a great extent as shown in the inset of Figure 1, while the monomer band was strengthened slightly with a clearer vibronic structure. This pH dependence is supposed to be related to the protonation–deprotonation

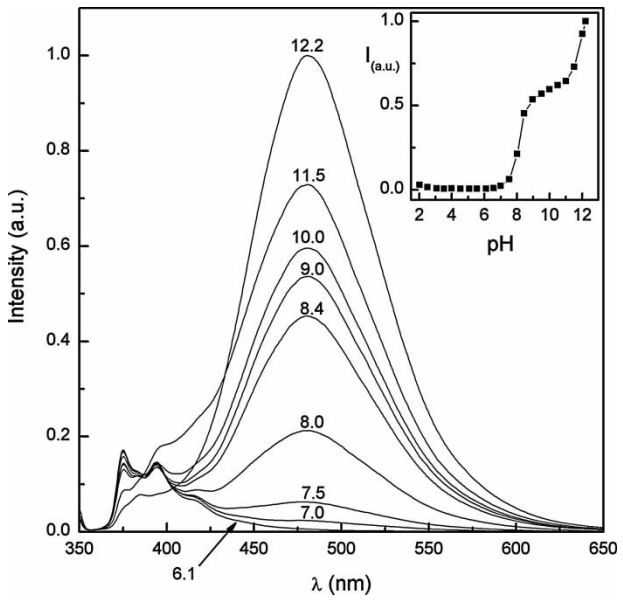

Figure 1. Emission spectra of (edtapy)H_2 in aqueous solution at selected pH values. The spectral intensities are normalised to the peak maximum of the most intense spectrum. The excitation wavelength, λ_{exc}, is 342 nm, and the concentration is 2×10^{-6} M. *Inset*: emission intensity (a.u.) at 490 nm as a function of pH; the solid line is drawn as an aid to visualising the intensity change.

equilibrium. The NMR study of a related naphthyl–EDTA compound, **3** in Scheme 1, has shown that the first protonation occurs at amino nitrogen of the EDTA chain with a logarithmic equilibrium constant of 7.84 between M^{2-} and MH^{-} species, and the second protonation occurs at carboxylate oxygen below pD 5.5 to form MH_2 species (*17*); this protonation scheme is basically identical with that reported for EDTA and its bis(amide) derivatives (*19*, *20*, *22*, *23*). The first protonation on $(edtapy)^{2-}$ is, therefore, supposed to occur at amino nitrogen to form $(edtapy)H^{-}$ around pH 8. A consequent conformational change is responsible for the regular sigmoid response observed in a pH region of 6–9 (Figure 1). The second protonation occurs at carboxylate oxygen to form $(edtapy)H_2$ at pH below 5, but no spectral change is observed in the acidic region (Figure 1).

Since the EDTA unit is completely deprotonated above pH 10, the second sharp change in emission intensity above pH 10 is attributable to the amide group, whose electronic structure and conformation are sensitively influenced by environmental changes (*24*). Especially, amide hydrogen is susceptible to pH in a strongly basic region because of its weak acidity. Even a small change in the electronic structure of the amide group results in a large influence on the emission from the chromophoric unit because it is directly bonded to the amide group. The sharp intensity profile against pH windows in two pH regions suggests that this EDTA–pyrene derivative may be a promising pH sensor in strongly basic solutions even at pH as high as 12 or above.

Pyrene excimers are classified into two categories on the basis of the origin, i.e. a dynamic excimer and a static excimer; the former originates from a pyrene dimer formed in the excited state and the latter is due to a pyrene dimer preformed in the ground state (*25*). A simple method to distinguish between them is the inspection of the absorption and excitation spectra: when pyrene is preassociated in the ground state, the absorption bands are broadened (sometimes accompanied by a small red shift and hypochromism) with reference to the spectrum of molecularly diluted pyrene, and more definitively, the excitation spectrum monitored by the excimer band undergoes a red shift and line broadening when compared with that monitored by the monomer band (*25*). Figure 2 shows the excitation spectra monitored at 480 nm (corresponding to the excimer emission peak) and 375 nm (the monomer emission peak) at different pH values. The excitation spectrum related to the excimer emission is intensified with increasing pH, and the spectrum related to the monomer emission is weakened; these pH dependences are correlated with those observed for the emission spectra. The spectral patterns of the two series of spectra are clearly different from each other. The difference is pronounced in the spectral region 300–400 nm: the monomer-related band at 330 nm is

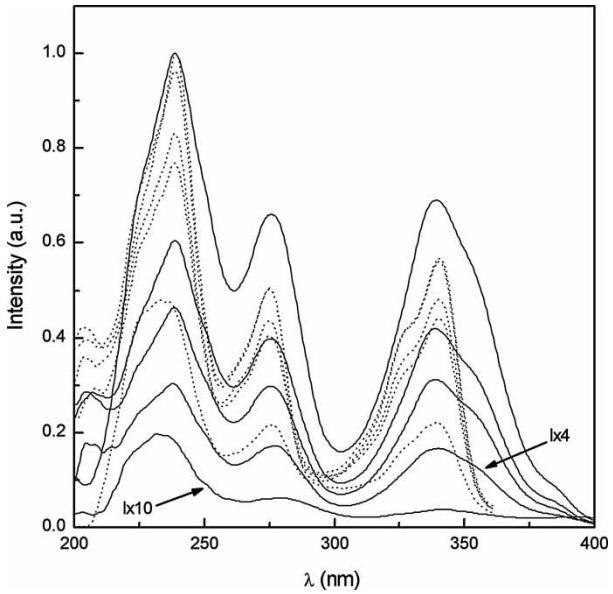

Figure 2. Excitation spectra of $(edtapy)H_2$ observed for emission bands at 375 (dotted line) and 480 nm (solid line) in aqueous solution at different pH values; pH is 12.2, 10, 8.4, 7.5 and 6.1 from the top to the bottom for the observation at λ_{em} 480 nm; the order of pH is reversed for the 375 nm observation. The concentration is 2×10^{-6} M. In each set of spectra, the spectrum intensities are normalised to the highest peak of the strongest spectrum.

accompanied by a shoulder at the shorter wavelength side; by contrast, the corresponding excimer-related band has a shoulder at the longer wavelength side so that the overall band undergoes a red shift and also a line broadening when compared with the monomer-related band. The absorption bands are slightly broadened with increasing pH and the structure is partially collapsed at high pH, although the intensity is enhanced (Figure S1 in Supplementary materials). These findings, especially those for the emission spectra, indicate that the emission at 480 nm is due to a static excimer formed as a result of preorganisation of the molecular conformation in the ground state.

Geometries and excimer formation in $(edtapy)^{2-}$ and $(edtapy)H^{-}$

With the objective of confirming the formation of a static excimer, geometry optimisation was carried out for $(edtapy)^{2-}$, which is the molecular species formed at high pH values, on the basis of DFT, with the B3LYP/6-31G(d) basis set implemented in Gaussian 03 (*26*). All geometry optimisations were followed by frequency calculations at the same level of the theory in order that the stationary points were characterised as true minima. The EDTA chain was short enough to be definitely

optimised. On the other hand, the carboxymethyl arms took various orientations with so small energy differences as to result in ambiguity in the geometry of the interlinking system, and negative charges on carboxylate oxygen caused additional difficulty in molecular modelling. For this reason, carboxymethyl groups were excluded in the geometry optimisation so that the true conformation was obtained readily and unequivocally for the chromophore–interlink–chromophore chain. The optimised model molecule was 1,4-bis(*N*-1-pyrenylacetamide)-1,4-diazabutane; its optimised geometry represents the conformation of the excimer-forming species $(edtapy)^{2-}$ in which the amino nitrogen atoms are neutral without being protonated. The obtained structure is displayed in Figure 3(A). Two pyrene rings orient almost parallel to each other with an angle of 5° between the ring planes, and are slipped away with a distance of 7.5 Å between the ring centres so as to form an edge-to-edge contact, which occurs at positions 8 and 9 with the following distances: $C(8)\cdots C(8') = 4.1$, $C(8)\cdots H(8') = 3.5$ and $H(8)\cdots H(8') = 3.1$ Å; $C(9)\cdots C(9') = 3.7$, $C(9)\cdots H(9') = 3.3$ and $H(9)\cdots H(9') = 3.3$ Å. Some of these distances are close to the corresponding van der Waals radius sums of aromatic-ring carbon (1.7 Å) and hydrogen (1.2 Å). In aqueous media, the two aromatic groups may become closer to each other to be overlapped with a shorter distance between the ring centres, because of the strong hydrophobic interaction (or solvent exclusion effect). The optimised structure of the model molecule suggests that an intramolecular pyrene pair can be definitely formed with a face-to-face stack in the ground state of $(edtapy)^{2-}$. This is consistent with the excitation spectra, interpreting the highly efficient excimer emission observed in basic solution.

As shown in Figure 3(B), a large conformational change occurs when an acidic proton is added onto one of the amino nitrogen atoms in the model molecule [N(2) in Figure 3(B)]. The angle between the ring plane is 44°; the distance between the ring centres amounts to 10.6 Å and the closest interatomic distances between the rings are as long as $C(9)\cdots C(9') = 7.3$, $C(9)\cdots H(9') = 6.6$ and $H(9)\cdots H(9') = 6.6$ Å; $C(10)\cdots C(10') = 7.1$, $C(10)\cdots H(10') = 6.4$ and $H(10)\cdots H(10') = 6.0$ Å. Thus, the pyrene rings are no longer parallel to each other and have no close contact either. This protonated model molecule represents the conformation of the pyrene–edtaH^+–pyrene linkage in $(edtapy)H^-$, in which the EDTA chain is protonated, and suggests that a static excimer is hardly formed in $(edtapy)H^-$ species. In addition, the presence of an acidic proton may cause another effect unfavourable for excimer formation as follows. Added proton leads to a hydrogen-bond formation between amino nitrogen N(2) and amide oxygen O(1); the interatomic distances in N(2)—H···O(1) are 1.1 and 1.8 Å, respectively. Since $(edtapy)^{2-}$ consists of two chemically equivalent moieties, the acidic proton in $(edtapy)H^-$ is exchanged between two amino nitrogen atoms [N(2) and N(3)]; in fact, the ^{1}H NMR spectra of similar EDTA derivatives show a single signal for equivalent CH_2 groups over an entire pH range studied (*17*, *19*, *20*, *22*, *23*). Concurrently with the proton exchange, the two moieties alternate their conformations. Such an internal molecular

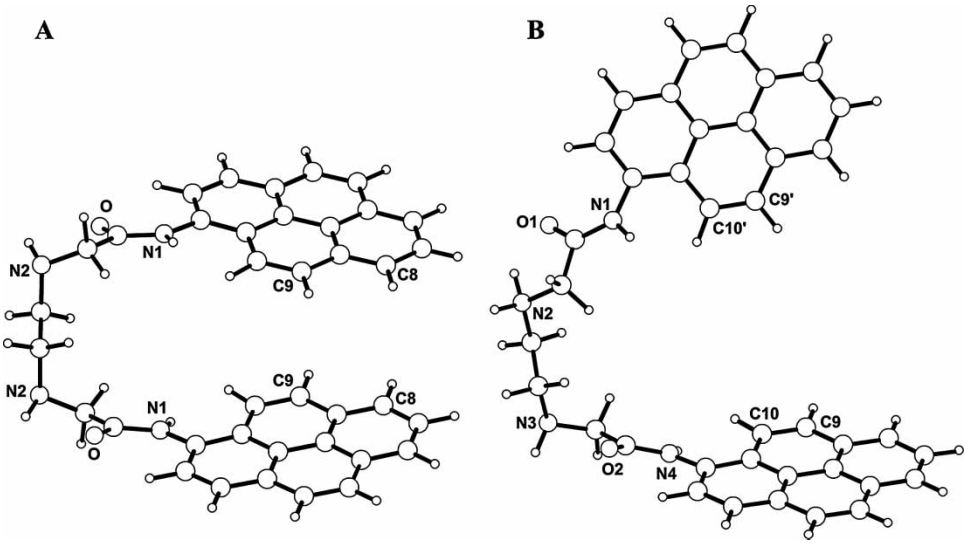

Figure 3. Geometries optimised on the basis of DFT with the B3LYP/6-31G(d) basis set for chromophore–interlink–chromophore systems in (A) $(edtapy)^{2-}$ and (B) $(edtapy)H^-$ species. Carboxymethyl groups were excluded for reliable optimisation of the linkage systems: the optimised model molecules are (A) 1,4-bis(*N*-1-pyrenylacetamide)-1,4-diazabutane and (B) its cationic molecule in which amino nitrogen N(2) is protonated. Structure A has a C_2 symmetry with an angle of 5° between the ring planes and a distance of 7.5 Å between the ring centres; in structure B, the angle between the ring planes is 44° and the distance between the ring centres is 10.6 Å.

motion may enhance an internal conversion rate (*3*), and a consequent decrease in the lifetime of the excited state is supposed to lower the chance of excimer formation. The DFT calculations evidently support that the sharp change in fluorescence intensity around pH 8 is caused by the geometrical difference between $(edtapy)^{2-}$ and $(edtapy)H^{-}$.

Luminescence of (dtpapy)H_3

The DTPA derivative **2**, $(dtpapy)H_3$, is more water soluble than the EDTA derivative **1** probably because of a larger number of hydrophilic units involved in the DTPA chain. The relatively high water solubility (about 0.5 mmol kg^{-1} in basic solution) facilitated characterisation, and made even ^1H NMR measurements possible in aqueous solution.

The emission spectra of $(dtpapy)H_3$ exhibited a broad band characteristic of pyrene excimers at 484 nm, and sharp peaks attributed to monomeric pyrene at 379 and 395 nm, as shown in Figure 4. The emission intensities of the monomer and excimer bands are plotted against pH in Figure 5. The intensity of the excimer band reached a maximum at pH 8 and a minimum at pH 10. This pH dependence is described as an off–on–off–on profile. By contrast, the monomer band is intensified steadily with increasing pH over the entire pH range studied, without showing a plateau or hump. The off–on–off–on profile is more clearly seen for the plot of the excimer-to-monomer

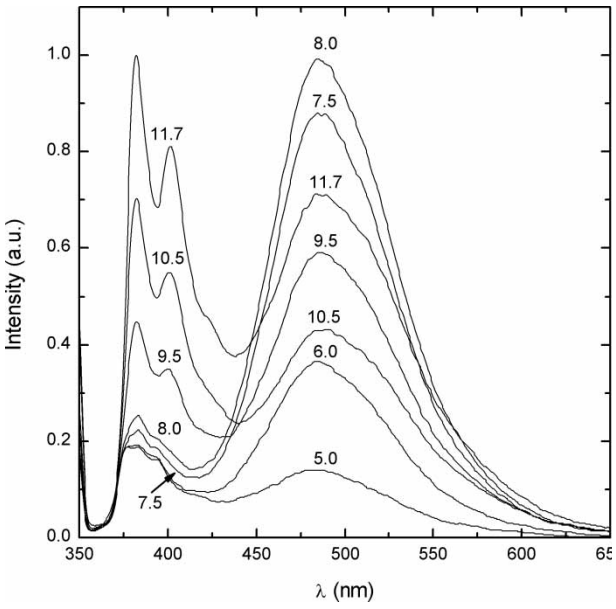

Figure 4. Emission spectra of $(dtpapy)H_3$ in aqueous solution at selected pH values. The spectral intensities are normalised to the peak maximum of the most intense spectrum. The excitation wavelength, λ_{exc}, is 342 nm, and the concentration is 1×10^{-6} M.

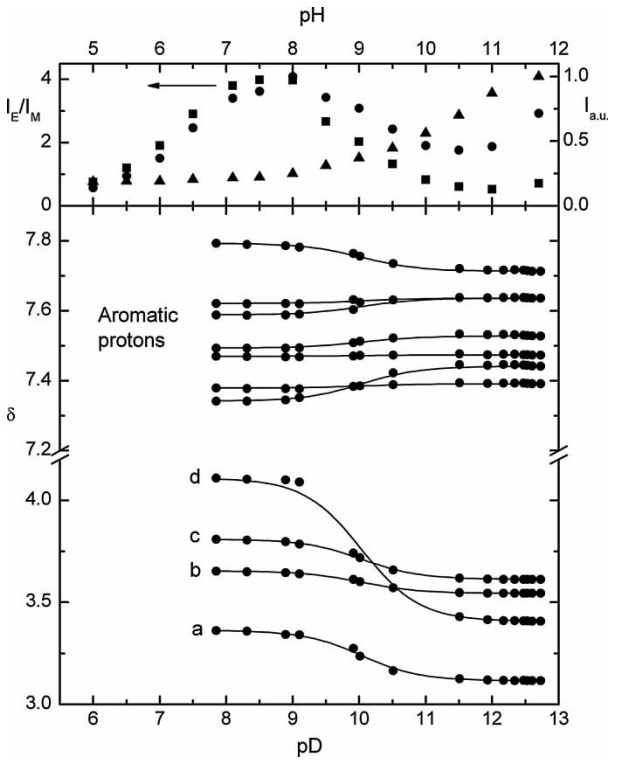

Figure 5. (Top) pH dependence of the emission intensity (a.u.) for $(dtpapy)H_3$: (circle) excimer emission intensity I_E; (triangle) monomer intensity I_M; (square) excimer-to-monomer intensity ratio I_E/I_M. I_E and I_M are intensities observed at 486 and 382 nm, respectively. (Bottom) pD dependence of the ^1H NMR chemical shifts (referenced to DSS) of $(dtpapy)H_3$. For the labels of CH_2 protons, see Scheme 1; aromatic protons are difficult to assign because of the complex spectral pattern under the influence of the magnetic field induced by the ring current of the other pyrene ring. The signal of proton 'd' was undetectable around pD 10 because of extreme-line broadening; below pD 7.5, the solubility was too low for NMR measurements. The solid lines were calculated by Equation (1), with $\log K_D = 10.04$. The scales of the pD and pH axes are displaced by one unit to facilitate the comparison of NMR (in D_2O) and fluorescence (in H_2O) data, because the pD value observed for a weak acid is about 0.8 higher than the corresponding pH value (*20*, *30*).

intensity ratio (Figure 5). These pH dependences of both excimer and monomer bands are quite different from those observed for the EDTA–pyrene derivative, providing an example for the important role of interlinking chains in bichromophores.

Figure 6 shows excitation spectra obtained at two emission wavelengths corresponding to the excimer and monomer emissions, respectively, at different pH values. The excimer-related band showed a maximum and a minimum in the intensity change with pH, while the monomer-related bands were steadily intensified with increasing pH. These pH dependences of the excitation bands are correlated with those of the corresponding emission bands. At pH 8, the excimer-related band is much

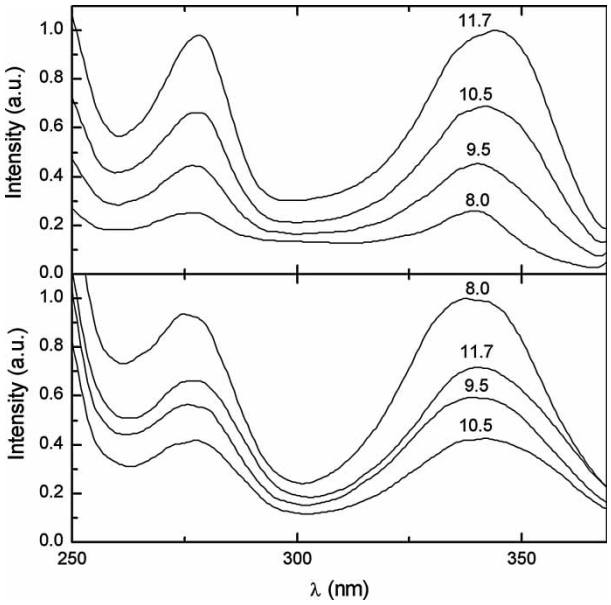

Figure 6. Normalised excitation spectra of $(dtpapy)H_3$ collected at (top) 382 and (bottom) 485 nm in aqueous solution at different pH values. The concentration is 1×10^{-6} M.

stronger than the monomer-related band, but their band maxima and band shapes are in a close resemblance. The monomer-related band shows a slight red shift with increasing pH, while such a shift with pH is not observed for the excimer-related band. Overall, the spectral pattern of the excimer-related spectra is essentially identical with that of the monomer-related spectra at every pH studied, in contrast to the EDTA derivative which shows a marked difference between the excimer- and monomer-related excitation spectra. The absorption spectrum in a region of 250–400 nm resembled the excitation spectra; the absorption bands were unchanged over the range pH $>$ 5, and were rather broadened below pH 5 (Figure S2 in Supplementary materials). These excitation and absorption spectra gave no evidence for the preassociation of the pyrenyl groups in the ground sate; probably, a dynamic excimer is formed in the excited state and responsible for the excimer emission, in contrast to the EDTA derivative. The geometry of the pyrene–DTPA–pyrene link could not be optimised because the DTPA unit had various conformations with very small differences in the energy minima, even when carboxylate arms were excluded from the optimisation. Obviously, however, DTPA chain is too long and flexible for the formation of a well-defined intramolecular face-to-face stack in the ground state; as a consequence, the excimer-to-monomer intensity ratio observed for the DTPA derivative is smaller than that of the EDTA derivative. The introduction of DTPA interlink results in the lower efficiency in excimer formation, but leads to the rare off–on–off–on profile.

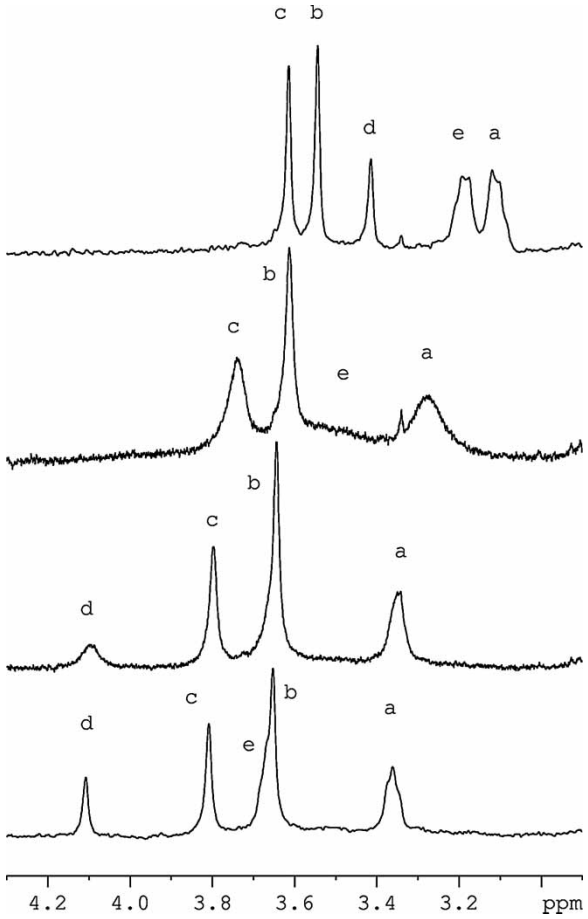

Figure 7. The ^{1}H NMR spectra of CH_2 protons of $(dtpapy)H_3$ at different pD values: from top to bottom pD = 11.9, 9.9, 8.9 and 7.9. For labelling, see Scheme 1. Protons 'd' and 'e' undergo line broadening so as to be undetectable at pD between 9.5 and 11.

^{1}H NMR of $(dtpapy)^{3-}$ and $(dtpapy)H^{2-}$: protonation and excimer formation

The ^{1}H NMR spectra of the CH_2 protons are shown in Figure 7 at selected pD values, and the δ values are plotted against pD in Figure 5. Every CH_2 proton undergoes a downfield shift with decreasing pD around pD 10, indicating that the first protonation–deprotonation process, i.e. the equilibrium between $(dtpapy)^{3-}$ and $(dtpapy)H^{2-}$, occurs around that pD value. The δ_j value of proton j is given by the following function of pD (*20*):

$$\delta_j(\mathrm{pD}) = \frac{\{\delta_{j0} + \delta_{j1} K_\mathrm{D} 10^{-\mathrm{pD}}\}}{\{1 + K_\mathrm{D} 10^{-\mathrm{pD}}\}}, \qquad (1)$$

Here, K_D is a protonation constant in D_2O, and δ_{j0} and δ_{j1} are the δ_j values of $(dtpapy)^{3-}$ and $(dtpapy)H^{2-}$, respectively. Curve fitting of the observed shifts with Equation (1) gave $\log K_\mathrm{D} = 10.04$. A comparison of the NMR and fluorescence data concludes that the emission intensity change observed in the pH range of 8–11 is

associated with the first protonation process, as seen in Figure 5, in which the scales of pD and pH are displaced by one unit as an aid for comparison because the pD value observed for a weak acid is about 0.8 higher than the corresponding pH value (*20*, *30*).

The largest shift upon protonation was observed for CH_2(d) and CH_2(e) bonded to the central amino nitrogen. In addition, these protons are broadened so as to be undetectable in the pD range of 9.5–11, as a result of a rapid exchange of the acidic hydrogen. These observations suggest that the first protonation occurs mainly at the central amino nitrogen to form (dtpapy)H^{2-}; hence, the second protonation occurs at one of the terminal amino nitrogen atoms at pD below 7.5, and (dtpapy)H_2^- is formed. This protonation scheme is consistent with that reported for DTPA and its bis(amide) derivatives (*22*, *23*, *27–29*). The change in fluorescence intensity around pH 9 is, therefore, caused by the protonation on the central amino nitrogen, and the fluorescence intensity change in the pH range of 5–8 is due to the protonation process on the terminal amino nitrogen.

Change in δ_j, $\Delta\delta_j$, of proton j in an $NCH_2(1)CH_2(2)$ unit is proportional to the proton population on the nitrogen, f_N (*22*):

$$\Delta\delta_j = C_j f_N \qquad (2)$$

Here, $\Delta\delta_j$ is the difference between the δ_j values before and after the protonation process, and C_j is the protonation shift constant of proton j. The protonation on the central amino nitrogen causes the δ change of proton 'a' as well as that of proton 'e', although the former is much smaller than the latter, but does not influence on proton 'b' because the protonation effect is rapidly attenuated in the course of propagation in the σ electron system (*23*). The observed change $\Delta\delta_b$ of proton 'b' suggests that a considerable proton population exists on the terminal amino nitrogen to which CH_2(b) is attached. On the basis of Equation (2), the ratio $\Delta\delta_b/\Delta\delta_d$ is equal to f_{Nt}/f_{Nc}, where subscripts 't' and 'c' stand for the terminal and central amino nitrogens, respectively. The total proton populations should be identical with the number of added acidic hydrogen atoms: $2f_{Nt} + f_{Nc} = 1$ for (dtpapy)H^{2-}. This restriction and the observed ratio, $\Delta\delta_b/\Delta\delta_d = 0.11/0.70$, give the populations as $f_{Nc} = 0.76$ and $f_{Nt} = 0.12$. These fractional populations suggest the formation of hydrogen bonding between the central and terminal nitrogen atoms in (dtpapy)H^{2-}, as schematically shown in Figure 8. The hydrogen bonding may fold the DTPA linkage in such a way that pyrene rings are close to each other, facilitating the formation of excimer at the excited state and resulting in the strong excimer emission observed around pH 8. In (dtpapy)H_2^-, two acidic hydrogen atoms added onto amino nitrogen undergo mutual electrostatic repulsion so as to populate over three amino nitrogen atoms (Figure 8), as concluded for DTPA and its derivatives (*22*, *23*). As a result, the DTPA chain is stretched so as to be unfavourable to excimer formation in (dtpapy)H_2^-. This conformational change upon protonation leads to the sharp change in the excimer emission observed at pH below 8.

Some pyrene-ring protons exhibit significant NMR shifts upon protonation (Figure 5), although the electronic structure of the pyrenyl group is not directly influenced by the protonation–deprotonation process on the central amino nitrogen. These NMR shifts are ascribable to the mutual ring-current effect on δ (or interannular interaction through space) because an aromatic ring generates an angle-dependent magnetic field on a nearby resonant proton (*31*, *32*). Hence, the observed pD dependence of the pyrene proton signals is evidence for a change in geometrical relation between two pyrene rings upon protonation, as shown in Figure 8.

Above pH 10.5, only a single species (dtpapy)$^{3-}$ exists with completely deprotonated amino nitrogen atoms; in fact, proton signals of any CH_2 groups bonded to amino nitrogen do not show a change in chemical shift above the corresponding pD value (Figure 5). Therefore, the fluorescence change observed at pH >11 is due to the sensitiveness of the amide group to environmental changes (*24*). The NMR data support that the incorporation of multiple amino and amide groups in the interlinking chain results in the off–on–off–on profile observed for the DTPA–pyrene bichromophore.

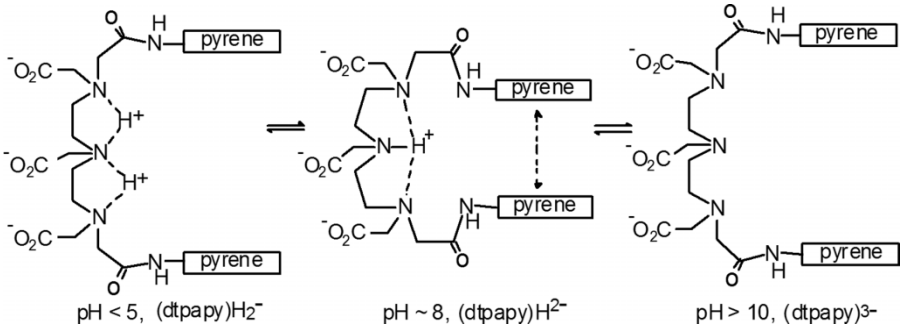

Figure 8. Protonation schemes and consequent conformational changes proposed for (dtpapy)H_n^{-3+n}. The hydrogen bonding in (dtpapy)H^{2-} may make the pyrene rings close enough to form excimer at the excited state.

Conclusion

The EDTA–pyrene bichromophore exhibits the sharp pH dependence of the excimer emission in two pH regions and the DTPA–pyrene bichromophore shows an off–on–off–on type of the pH–intensity profile. These pH-sensitive properties result from the interlinking chains that have multiple functional sites including amino and amide nitrogen atoms. The conformations of the amide-based polyamino chains are sensitively altered with protonation on amino nitrogen, and amide group contributes to the intensity profile against a pH window at extremely high pH values. These new bichromophores may meet the demand of pH sensors capable of detecting even a small pH change in a specific region; conspicuously, it works at pH as high as 12.

Experimental

Materials

EDTA dianhydride and 1-aminopyrene were supplied from Aldrich (Milwaukee, WI, USA) and DTPA dianhydride from Sigma (St Louis, MO, USA). All chemicals were used as received.

*Synthesis of (edtapy)H_2: 1,4-bis(methylenecarboxy)-1,4-bis(*N*-1-pyrenylacetamide)-1,4-diazabutane*

(Edtapy)H_2 was synthesised by adding solid EDTA dianhydride (0.31 g, 1.2 mmol) little-by-little through a powder-dispensing funnel to 1-aminopyrene (0.78 g, 3.6 mmol) dissolved in dimethylformamide (DMF, 15 ml), with stirring under a nitrogen atmosphere in an ice bath. The resulting reaction mixture was left to stand overnight at room temperature and then heated at 50°C for 4 h. Any solid present was removed by filtration and the filtrate was concentrated to a viscous liquid, to which 100 ml of acetone was added. When the resulting solution was left to stand in the dark for 3 days, a large quantity of pale green needle-like crystals were obtained, which were separated from the solution, washed with acetone and dried in vacuum. Recrystallisation from DMF by adding acetone was repeated until colourless crystals were obtained (0.32 g, 38%); mp 184°C (dec). ^{1}H NMR (400 MHz, DMSO-d_6, TMS): $\delta = 3.123$ (s, 4H, H_a), 3.689 (s, 4H, H_b), 3.701 (s, 4H, H_c) and 7.989–8.367 (m, 18H, ArH); MS (ESI) *m*/*z* (%): 691.1 (100) [$(M+H)^+$]; elemental analysis calcd (%) for $C_{42}H_{34}N_4O_6 \cdot 1.5C_3H_6O$: C, 71.80; H, 5.57; N, 7.20; found: C, 71.55; H, 5.51; N, 7.34.

*Synthesis of (dtpapy)H_3: 1,4,7-tris(methylenecarboxy)-1,7-bis(*N*-1-pyrenylacetamide)-1,4,7-triazaheptane*

This compound has recently been reported to be obtained as light brown solid, for preparing its lanthanide complexes, by a reaction in acetonitrile with triethylamine, followed by purification with a silica gel column (*21*). In our work, colourless product was obtained by the use of DMF as a solvent and recrystallisation from dimethlsulphoxide (DMSO)/acetone, as described below. Solid DTPA dianhydride (0.56 g, 1.6 mmol) was added little-by-little to 1-aminopyrene (1.0 g, 4.8 mmol) in DMF (15 ml) at room temperature with stirring under a nitrogen atmosphere. The resulting reaction mixture was left to stand overnight at room temperature and then heated at 50°C for 4 h. After filtration, the solution was concentrated to a viscous liquid. Addition of acetone (25 ml) to the concentrate yielded a pale green solid, which was separated by filtration and washed thoroughly with acetone. The solid was dried in vacuum and dissolved in DMSO. The resulting solution was concentrated to a minimum volume in a rotary evaporator, and, at once, acetone was carefully poured until covering the concentrate. The resulting solution was left to stand in the dark. In a week, crystals were formed in a large quantity. The crystals were separated from the solution, washed with acetone and dried in vacuum. The crystallisation from DMSO/acetone was repeated until colourless crystals were obtained (0.54 g, 43%); mp 156°C (dec). ^{1}H NMR (400 MHz, DMSO-d_6, TMS): $\delta = 3.056$ (t, 4H, $J = 5.55$, H_a), 3.593 (s, 4H, H_b), 3.608 (s, 4H, H_c), 3.451 (s, 2H, H_d), 2.984 (t, 4H, $J = 5.52$, H_e) and 7.980–8.413 (m, 18H, ArH); HRMS (FAB) *m*/*z* (%): 792.2935 (100) $(M+H)^+$; elemental analysis calcd (%) for $C_{46}H_{41}N_5O_8 \cdot 2.5H_2O$: C, 66.02; H, 5.50; N, 8.37; found: C, 66.08; H, 5.51; N, 8.43.

Spectroscopic measurements

Luminescence spectra were recorded on a Perkin-Elmer LS-50B luminescence spectrometer. For experiments of pH dependence, sample compounds were dissolved in 0.01 M NaCl solution by adding an equimolar amount of solid Na_2CO_3, and the pH values of the sample solutions were adjusted by using 0.01 M HCl and 0.01 M NaOH, so that the ionic strength was kept constant. Absorption spectra were obtained with a Perkin-Elmer Lambda 20 UV–vis spectrometer. Sample solutions were prepared by the same procedure as for the fluorescence measurements. The ^{1}H NMR spectra were obtained with a Brucker AVANCE 400 spectrometer at a probe temperature of approximately 23°C. The studies of pD dependence of (dtpapy)H_3 in D_2O were carried out at a concentration of 0.5 mmol kg^{-1} in the pD range of 7.9–12.7. Below the former pD, the water solubility was too low for reliable NMR experiments. Two stock solutions (0.5 mmol kg^{-1}) were prepared by adding a minimal amount of solid Na_2CO_3 into suspension of (dtpapy)H_3 in D_2O containing 0.01% DSS (sodium 2,2-dimethyl-2-silapentane-5-sulphonate) as the internal reference, followed by adjusting the pD to the lowest and the highest values with dilute

solutions of HCl-d and KOH-d in D_2O, respectively. Sample solutions were prepared by weighing out the stock solutions directly into NMR sample tubes in different ratios in such a way that the total weight of every sample solution was 0.5 g. The pD value of a sample solution was determined by inserting an Aldrich ultra-thin long-stem combination electrode into the sample tube after recording NMR. The electrode was calibrated with standard aqueous buffers in advance, and a pH value measured with a Corning 440 pH meter was converted to the pD value on the basis of the relation $pD = pH_{meas} + 0.45$ (*33*). The EDTA derivative has a very low water solubility ($< 0.1\,mmol\,kg^{-1}$) for reliable NMR experiments in D_2O. The mass spectra were obtained for NH_3–methanol solutions at the University of Arizona Mass Spectroscopy Facility (Tucson, AZ, USA) and by using a high-resolution Jeol MStation 700 spectrometer in FAB technique at the Universidad Autónoma del Estado de Morelos (Cuernavaca, Morelos, México). The elemental analyses were performed by Desert Analytics (Tucson, AZ, USA).

Acknowledgements

This work was supported in part by the Consejo Nacional de Ciencia y Tecnología de México (CONACYT, Project No. 489100-5-J35194-N). The NMR spectrometer is operated under the support of the Secretaría de Educación Publica, México (SESIC-SEP, Programme Nos. P/PIFI 2005-26-12 and P/PEF 2005-26-11). The authors thank Karla Y. Herrera Valenzuela for the technical assistance. R.P.-G. is indebted to CONACYT for graduate scholarship.

References

(1) Czarnik, A.W. *Fluorescence Chemosensors for Ion and Molecule Recognition*; American Chemical Society: Washington, DC, 1992.
(2) Pietraszkiewicz, M. In *Supramolecular Technology: Comprehensive Supramolecular Chemistry*; Reinhoudt, D.N., Ed.; Pergamon-Elsevier: New York, 1996; Vol. 10, p 225.
(3) Valeur, B. *Molecular Fluorescence*; Wiley-VCH: Weinheim, 2002.
(4) Kawakami, J.; Komai, Y.; Sumori, T.; Fukushi, A.; Shimozaki, K.; Ito, S. *J. Photochem. Photobiol. A* **2001**, *139*, 71–78.
(5) Kawakami, J.; Fukushi, A.; Ito, S. *Chem. Lett.* **1999**, *28*, 955–956.
(6) Albelda, M.T.; Bernardo, M.A.; Díaz, P.; García-España, E.; Seixas de Melo, J.; Pina, F.; Soriano, C.; Luis, S.V. *Chem. Commun.* **2001**, 1520–1521.
(7) Albelda, M.T.; García-España, E.; Gil, L.; Seixas de Melo, J.; Pina, F.; Soriano, C.; Luis, S.V. *J. Phys. Chem. B* **2003**, *107*, 6573–6578.
(8) Alarcón, J.; Aucejo, R.; Albeda, M.T.; Alves, S.; Clares, M.P.; García-España, E.; Lodeiro, C.; Marchin, K.L.; Parola, A.J.; Pina, F.; Seixas de Melo, J.; Soriano, C. *Supramol. Chem.* **2004**, *16*, 573–580.
(9) Suzuki, Y.; Morozumi, T.; Nakamura, H.; Shimomura, M.; Hayashita, T.; Bartsh, R.A. *J. Phys. Chem. B* **1998**, *102*, 7910–7917.
(10) Yang, J.-S.; Lin, C.-S.; Hwang, C.-Y. *Org. Lett.* **2001**, *3*, 889–892.
(11) Sancenón, F.; Descalzo, A.B.; Lloris, J.M.; Martínez-Máñez, R.; Pardo, T.; Seguí, M.J.; Soto, J. *Polyhedron* **2002**, *21*, 1397–1404.
(12) Kakizawa, Y.; Akita, T.; Nakamura, H. *Chem. Lett.* **1993**, 1671–1674.
(13) Sclafani, J.A.; Maranto, M.T.; Sisk, T.M.; Van Arman, S.A. *Tetrahedron Lett.* **1996**, *37*, 2193–2196.
(14) Van Arman, S.A.; Sisk, T.M.; Zawrotny, D.M. *Lett. Org. Chem.* **2005**, *2*, 54–56.
(15) Shiraishi, Y.; Tokitoh, Y.; Hirai, T. *Org. Lett.* **2006**, *8*, 3841–3844.
(16) Shiraishi, Y.; Tokitoh, Y.; Nishimua, G.; Hirai, T. *J. Phys. Chem. B* **2007**, *111*, 5090–5100.
(17) Machi, L.; Santacruz, H.; Sánchez, M.; Inoue, M. *Supramol. Chem.* **2006**, *18*, 561–569.
(18) Machi, L.; Santacruz, H.; Sánchez, M.; Inoue, M. *Inorg. Chem. Commun.* **2007**, *10*, 547–550.
(19) Inoue, M.B.; Munoz, I.C.; Inoue, M.; Fernando, Q. *Inorg. Chim. Acta* **2000**, *300–302*, 206–211.
(20) Inoue, M.B.; Machi, L.; Munoz, I.C.; Rojas-Rivas, S.; Inoue, M.; Fernando, Q. *Inorg. Chim. Acta* **2001**, *324*, 73–80.
(21) Pope, S.J.A. *Polyhedron* **2007**, *26*, 4818–4824.
(22) Sudmeier, J.L.; Reilley, C.N. *Anal. Chem.* **1964**, *36*, 1698–1706.
(23) Inoue, M.B.; Oram, P.; Inoue, M.; Fernando, Q. *Inorg. Chim. Acta* **1995**, *232*, 91–98.
(24) Stewart, W.E.; Siddall, T.H., III. *Chem. Rev.* **1970**, *70*, 517–551.
(25) Winnik, F.M. *Chem. Rev.* **1993**, *93*, 587–614.
(26) Frisch, M.J.; Trucks, G.W.; Schlegel, H.B.; Scuseria, G.E.; Robb, M.A.; Cheeseman, J.R.; Montgomery, J.A., Jr.; Vreven, T.; Kudin, K.N.; Burant, J.C.; Millam, J.M.; Iyengar, S.S.; Tomasi, J.; Barone, V.; Mennucci, B.; Cossi, M.; Scalmani, G.; Rega, N.; Petersson, G.A.; Nakatsuji, H.; Hada, M.; Ehara, M.; Toyota, K.; Fukuda, R.; Hasegawa, J.; Ishida, M.; Nakajima, T.; Honda, Y.; Kitao, O.; Nakai, H.; Klene, M.; Li, X.; Knox, J.E.; Hratchian, H.P.; Cross, J.B.; Bakken, V.; Adamo, C.; Jaramillo, J.; Gomperts, R.; Stratmann, R.E.; Yazyev, O.; Austin, A.J.; Cammi, R.; Pomelli, C.; Ochterski, J.W.; Ayala, P.Y.; Morokuma, K.; Voth, G.A.; Salvador, P.; Dannenberg, J.J.; Zakrzewski, V.G.; Dapprich, S.; Daniels, A.D.; Strain, M.C.; Farkas, O.; Malick, D.K.; Rabuck, A.D.; Raghavachari, K.; Foresman, J.B.; Ortiz, J.V.; Cui, Q.; Baboul, A.G.; Clifford, S.; Cioslowski, J.; Stefanov, B.B.; Liu, G.; Liashenko, A.; Piskorz, P.; Komaromi, I.; Martin, R.L.; Fox, D.J.; Keith, T.; Al-Laham, M.A.; Peng, C.Y.; Nanayakkara, A.; Challacombe, M.; Gill, P.M.W.; Johnson, B.; Chen, W.; Wong, M.W.; Gonzalez, C.; Pople, J.A. Gaussian 03, Revision E.01; Gaussian, Inc.: Wallingford, CT, 2004.
(27) Kula, R.J.; Sawyer, D.T. *Inorg. Chem.* **1964**, *3*, 458.
(28) Letkeman, P.; Martell, A.E. *Inorg. Chem.* **1979**, *18*, 1284–1289.
(29) Inoue, M.B.; Santacruz, H.; Inoue, M.; Fernando, Q. *Inorg. Chim.* **1999**, *38*, 1596–1602.
(30) Bates, R.G. *Anal. Chem.* **1968**, *40* (6), 28A–37A.
(31) Pople, J.A.; Schneider, W.G.; Bernstein, H.J. *High-resolution Nuclear Magnetic Resonance*; McGraw-Hill: New York, 1959; p 180.
(32) Johnson, C.E., Jr.; Bovey, F.A. *J. Chem. Phys.* **1958**, *29*, 1012–1014.
(33) Covington, A.K.; Paabo, M.; Robinson, R.A.; Bates, R.G. *Anal. Chem.* **1968**, *40*, 700–706.